Polymer Chemistry

Cite this: *Polym. Chem.*, 2011, **2**, 2818

www.rsc.org/polymers

PAPER

Facile synthesis of cross-linked patchy fluorescent conjugated polymer nanoparticles by click reactions†

Vüsala İbrahimova, Seyma Ekiz, Özlem Gezici and Dönüs Tuncel*

Received 22nd July 2011, Accepted 16th September 2011
DOI: 10.1039/c1py00332a

Here, we report a novel method to synthesize multifunctional nanoparticles that can be used in biological studies, such as in cell imaging and as a carrier for biomolecules/drugs. The nanoparticles were prepared either *via* Cu-catalyzed or cucurbit[6]uril (CB6)-catalyzed click reactions between azide groups containing hydrophobic blue, green and yellow emitting fluorene-based conjugated polymers and a hydrophilic diaminodialkyne containing cross-linker. Through the click reaction, not only does the cross-linking confer stability, but it also introduces functional groups, such as triazoles and amines, to the nanoparticles. Moreover, CB6 not only acted as a catalyst to facilitate the copper-free click reaction, but it also allowed us to obtain nanoparticles containing rotaxanes in which the triazole units were encapsulated by CB6 units. TEM images of the nanoparticles also showed that they display very interesting morphologies. Incorporation of hydrophilic functional groups to the hydrophobic conjugated polymers resulted in a distinct phase separation, producing Janus-like or patchy particles.

Introduction

Conjugated polymer-based, water-dispersible nanoparticles are emerging as a new class of fluorescent probe for cell imaging and tracking because they offer high brightness, improved photostability, high fluorescent quantum yields and non-cytotoxicity compared to conventional dyes and quantum dots.[1–12] Moreover, judicious modification of the conjugated polymers employed allows one to synthesize stable multifunctional nanoparticles that can be suitable for theranostic nanomedicine, in which the agents for diagnosis and therapy can be loaded on the same nanoparticle.[13]

Conjugated polymer nanoparticles (CPNs) can be mainly prepared by mini-emulsion[1] and re-precipitation methods.[2] The mini-emulsion method involves the use of surfactants and hydrophobes. However, the re-precipitation method does not require the use of surfactants. In this method, the polymer is dissolved in a water miscible solvent and the resulting polymer solution is injected into a large amount of water, which is a poor solvent for the polymer. After the removal of the organic solvent, conjugated polymer nanoparticles are obtained. Although there are some recent examples involving the use of capping agents that allows attachment of the CPNs to a biological entity,[7b,8–10] these examples are quite scarce and most of the works are based on the hydrophobic conjugated polymers carrying no functional groups to be further modified. Another drawback preventing the exploitation of CPNs is the mechanical instability of these nanoparticles. To this end, the development of mechanically stable and multifunctional CPNs are highly sought after for many applications, such as in the area of biomedicine and photonics. In this context, recently we reported a method to prepare mechanically stable CPNs using a conjugated polymer with cross-linkable azide functional groups. These groups decomposed under light to create networks around the core to confer stability to the CPNs.[14]

Here, we adopt a novel method to synthesize cross-linked patchy fluorescent conjugated polymer nanoparticles. This method involves the use of a 1,3-dipolar cycloaddition reaction between azide and alkyne functional groups using Cu(I) or cucurbit[6]uril (CB6) as catalysts. Through the 1,3-dipolar cycloaddition, not only is cross-linking obtained, which confers stability, but functional groups, such as triazoles and amines, are introduced to the nanoparticles. In this method, it could be possible to use much higher concentrations of the polymers than the simple precipitation method because the resulting nanoparticles are shape persistent and resist coalescing. Moreover, the positive charges on the nanoparticles introduced *via* cross-linking will cause repulsion of the nanoparticles and will stabilize them without the need for surfactants. We wished to use CB6 in the nanoparticle synthesis because of a number of reasons. Cucurbiturils are highly versatile macrocycles that can be used in many applications.[15] They have a hydrophobic cavity, along with two matching hydrophilic carbonyl portals. CB6 has been shown to catalyze 1,3-dipolar cycloadditions between properly functionalized alkyne and azide groups to yield 1,4-disubstituted

Department of Chemistry and Institute of Material Science and Nanotechnology, Bilkent University, 06800 Ankara, Turkey. E-mail: dtuncel@fen.bilkent.edu.tr

† Electronic Supplementary Information (ESI) available: synthetic details of the monomers, characterization data, NMR spectra, DLS histographs, TEM images and UV–Vis and PL spectra. See DOI: 10.1039/c1py00332a

triazoles. Using these features, a number of rotaxanes and polyrotaxanes have been designed and synthesized.[16] Here, by taking advantage of this characteristic of CB6, pH-responsive rotaxane-containing nanoparticles are prepared. Furthermore, the use of CB6 allowed us to perform copper-free click reactions; this aspect is highly valuable because the presence of even trace amounts of cytotoxic copper is not desirable in biological studies.

Results and discussion

In the nanoparticle synthesis, we utilized three types of conjugated polymer containing azide functional groups, namely, poly[(9,9-dihexylfluorene)-*co*-9,9-bis(6-azidohexyl)fluorene)] (**P1**), poly[(9,9-dihexylfluorene)-*co*-(2,5-(2-azidoethylthiophene)] (**P2**) and poly[9,9-bis(3-azidopropyl)fluorene)-*co*-(4,7-benzothiodiazole)] (**P3**). The structures of the polymers **P1–P3** are shown in Scheme 1.

The synthesis of **P1** has been reported elsewhere.[17] The precursor polymer of **P2** was synthesized by the Suzuki coupling of 2,5-dibromo-3-(2-bromoethyl)-thiophene[18] with 9,9-dihexylfluorene-2,7-bis(trimethyleneborate) and then the bromide groups were converted into the azide by a nucleophilic substitution reaction using sodium azide in DMF to yield **P2**. To synthesize **P3**, first poly[9,9-bis(3-bromopropyl)fluorene)-*co*-(4,7-benzothiodiazole)] was synthesized by the Suzuki coupling of 2,1,3-benzothiadiazole-4,7-bis(boronic acid pinocol ester) and 2,7-dibromo-9,9-bis(3-bromopropyl)-9*H*-fluorene and, subsequently, the bromide groups were substituted by azides to afford **P3** (ESI, Scheme S1–S2†). The conversion of the bromide groups to azides was verified by ^{1}H-NMR and FT-IR spectroscopy. The characteristic azide bond stretching at 2094 cm^{-1} was observed by FT-IR (ESI, Figure S1†). The weight average molecular weights (M_w) were determined as 2.1×10^4 g mol^{-1}, 3.9×10^3 g mol^{-1} and 1.1×10^4 g mol^{-1} for **P1**, **P2** and **P3**, respectively, by gel permeation chromatography (GPC) using polystyrene as a standard.

Two sets of nanoparticles were prepared using polymers **P1**, **P2** and **P3** with two different procedures. Nanoparticles synthesized by a Cu(I)-catalyzed click reaction were abbreviated to **P1-CPNa**, **P2-CPNa** and **P3-CPNa** and CB6-catalyzed nanoparticles were abbreviated to **P1-CPNb**, **P2-CPNb** and **P3-CPNb**. In a typical nanoparticle synthesis, the polymer was dissolved in a good solvent, such as THF, and the filtered solution was injected into the diaminoalkyne (*N*,*N*′-di-prop-2-ynyl-propane-1,3-diamine hydrochloride),[16c] with the catalyst, either Cu(I) ($CuSO_4$ and sodium ascorbate) or CB6 containing water, whilst sonicating. After injection of the polymer solution, the mixture was left overnight at room temperature and, subsequently, the THF was removed under reduced pressure and the remaining solution was dialyzed in water using a 14 kDa cut-off regenerated cellulose membrane for 24 h to remove the catalyst and any unreacted diaminoalkyne. Clear solutions were obtained with a polymer content of 5×10^{-2} mg ml^{-1}. While Fig. 1a illustrates a cartoon representation of the synthesis of the CPNs *via* Cu(I)-catalyzed or CB6-catalyzed click reactions, Fig. 1b shows the detailed structures, which can form through inter- or

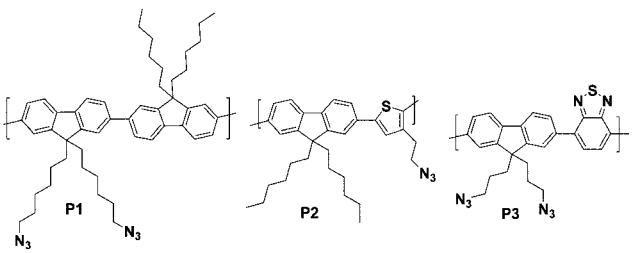

Scheme 1 Molecular structures of polymers P1, P2 and P3 used in the nanoparticle synthesis.

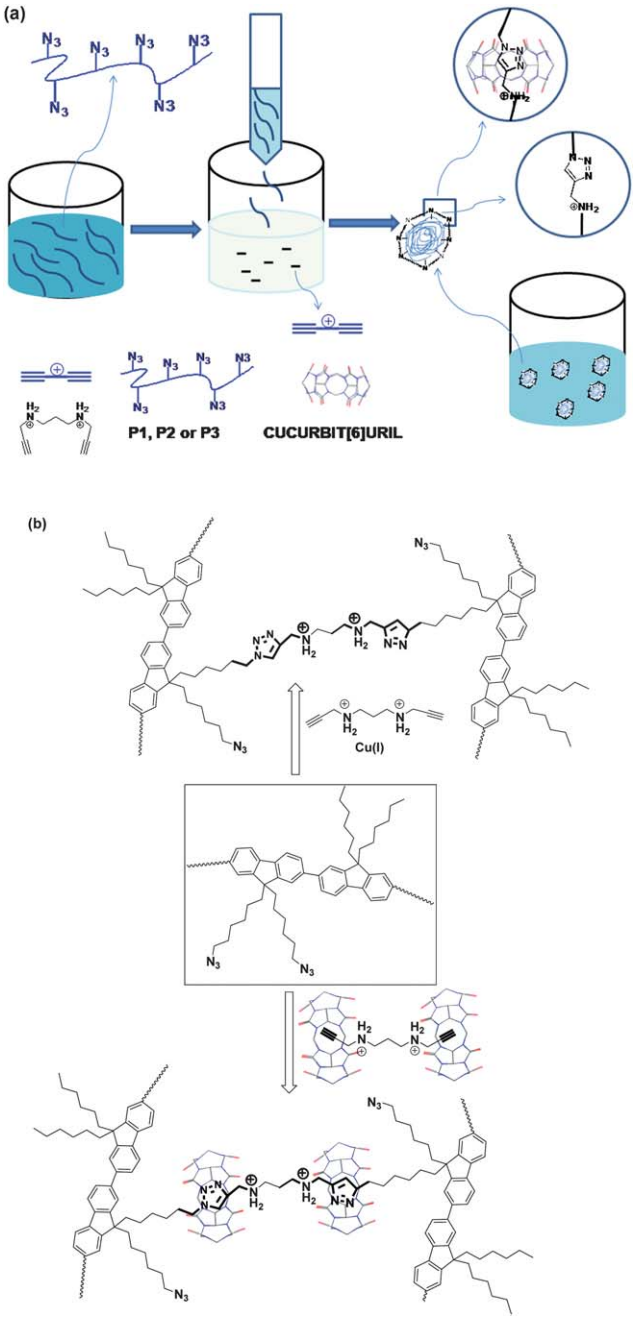

Fig. 1 (a) A cartoon representation of the synthesis of the CPNs *via* Cu(I)-catalyzed or CB6-catalyzed click reactions; (b) detailed structures of the cross-linking of **P1** through the Cu(I)-catalyzed or CB6-catalyzed click reactions. This also shows the structure of the rotaxanes formed through the CB6-catalyzed click reaction.

intra- cross-linking. Rotaxane formation through the CB6-catalyzed click reaction involves, first, the formation of a ternary complex between the diaminoalkyne, the azide and CB6. The proper alignment of the azide and the alkyne groups inside the cavity of CB6 induces triazole formation.[16f] CB6 prefers to encapsulate the triazoles at a low pH due to ion–dipole interactions between ammonium ions and the carbonyl groups of CB6. By deprotonating the ammonium ions at a high pH, it is possible to change the location of CB6.

The optical properties of polymers **P1**, **P2** and **P3** in THF and the nanoparticle dispersions in water were investigated by UV–vis absorption and emission spectroscopy and their spectra are displayed in Fig. 2 (for the enlarged spectra, see the ESI†). Converting the polymers into nanoparticles caused some changes in the absorption and emission properties of the nanoparticles, as observed in previous studies.[2–14] For example, red-shifts in the absorption wavelengths for **P1-CPNa** ($\Delta\lambda = 5$ nm), **P2-CPNa** ($\Delta\lambda = 10$ nm) and **P3-CPNa** ($\Delta\lambda = 11$ and 21 nm) were observed. Red-shifts were also observed in the emission wavelengths of the nanoparticle dispersions compared to the polymer solutions in THF, which are most significant for **P2-CPNa** ($\Delta\lambda = 55$ nm) and **P3-CPNa** ($\Delta\lambda = 20$ nm) than **P1-CPNa** ($\Delta\lambda = 3$ and 4 nm).

The observed red-shifts in the absorption and emission spectra of the nanoparticles compared to the polymer solutions in THF can be attributed to the chain–chain interactions caused by π–π stacking of the polymer chains as well as the polarity differences in the solvents. These behaviors resemble the optical properties of the polymers in their bulk state, where the chain–chain interactions are highly extensive as shown in Fig. 2 and Table 1.

Some changes were also observed in the absorption and emission wavelengths (λ) of CB6-containing nanoparticles with respect to the spectra of the polymers in THF. For example, the absorption wavelengths (λ) of **P1-CPNb**, **P2-CPNb** and **P3-CPNb** have been observed at 395 nm, 394 nm, and 323, 447 nm, respectively. The emission wavelengths (λ) of the nanoparticle dispersions in water, compared to polymer solutions in THF, red-shifted about 3–4 nm, 35 nm and 3 nm for **P1-CPNb**, **P2-CPNb** and **P3-CPNb**, respectively. As can be seen, these changes are less significant when compared to the red-shifts observed in the wavelengths of the Cu(I)-catalyzed nanoparticles, indicating that the presence of the bulky CB6 units helps to isolate the individual polymer chains by decreasing the chain–chain interactions.

The fluorescence quantum yields of the polymers in THF and the nanoparticle dispersions were measured and are shown in Table 1. If we compare the fluorescence quantum yields of **P1-CPNa**, **P2-CPNa** and **P1-CPNa** with **P1-CPNb**, **P2-CPNb**

Table 1 The optical properties of polymers **P1–P3** in THF solutions and their nanoparticle dispersions in water[a]

	λ_{abs} (nm)	λ_{em} (nm)	Φ_f (%)
P1	390	422, 447	83
P2	382	457	83
P3	319, 442	552	82
P1 (film)	382	428, 452	Not determined
P2 (film)	385	505	Not determined
P3 (film)	321, 451	556	Not determined
P1-CPNa	395	426, 451	11
P2-CPNa	392	512	2
P3-CPNa	330, 463	572	5
P1-CPNb	395	426, 450	8
P2-CPNb	394	492	3
P3-CPNb	323, 447	555	5

[a] λ_{abs}: wavelength of the absorption maximum, λ_{em}: wavelength of the emission maximum, Φ_f: fluorescence quantum yield. Fluorescence quantum yields for **P1** and its nanoparticle dispersions were measured against quinine sulfate, which has a quantum yield of 0.5 in 0.1 M H_2SO_4. For **P2**, **P3** and their nanoparticles, fluorescein was used as a standard, which has a quantum yield of 0.98 in ethanol.

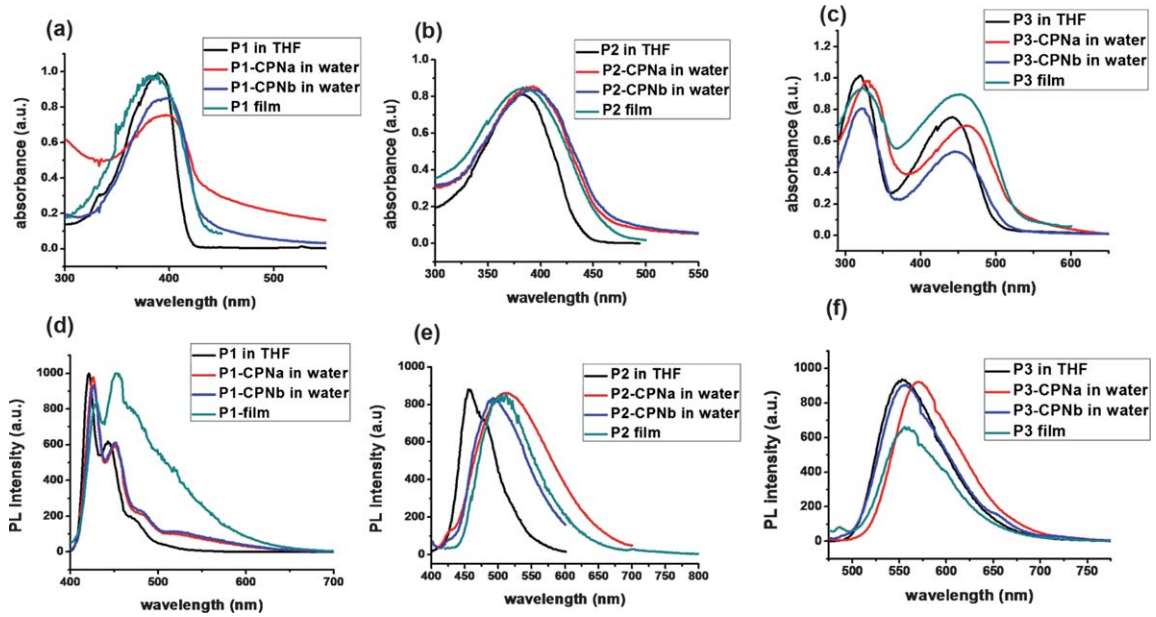

Fig. 2 UV–vis absorption spectra of **P1–P3** in THF, as films and as dispersions of the nanoparticles in water (**P1-CPNa**, **P2-CPNa**, **P3-CPNa**, **P1-CPNb**, **P2-CPNb** and **P3-CPNb**) (a, b, c) and the emission spectra of **P1–P3** in THF, as films and as dispersions of the nanoparticles in water (**P1-CPNa**, **P2-CPNa**, **P3-CPNa**, **P1-CPNb**, **P2-CPNb** and **P3-CPNb**) (d, e, f).

and **P1-CPNa**, we can see that there are no significant differences between them. However, as can be expected, overall the CPNs have lower fluorescence quantum yields than the polymer solutions in organic solvents. This indicates that the emission intensity is decreased mainly due to increasing competitive non-radiative decay processes, arising from an increased number of polymer chains in close contact with each other.

The dynamic light scattering (DLS) measurements were taken to determine the hydrodynamic size of the CPNs. Table 2 summarizes the particle sizes and polydispersity index values of the nanoparticles. Although the concentration of the polymers and the diazide were kept almost the same for both methods, the Cu(I)-catalyzed click reaction yielded bigger nanoparticles than the CB6-catalyzed click reaction; this is more noticeable for the nanoparticles of **P1**and **P3**. This can be attributed to the reactivity differences of the catalysts used for these reactions. It seems that the former reaction is faster and the intermolecular cross-linking is more dominant than in the latter.

Nanoparticles were also examined using transmission electron microscopy (TEM). The TEM images indicated that the nanoparticles exhibited interesting morphologies as shown in Fig. 3 and 4 (for more images, see the ESI†). It seems that the cross-linking of the azide groups of the polymers with hydrophilic diaminoalkyne through a 1,3-dipolar cycloaddition causes a phase separation and, as a result, Janus-like or patchy particles form.[19] Janus-like particles are non-centrosymmetric particles; this feature arises from the distribution of the functional groups with different reactivity and polarity over the particle surfaces. These kinds of nanoparticles are getting an increasing amount of attention because of their potential applications in advanced technologies, including theranostic nanomedicine and as sensors. Among many methods, their synthesis through the self-assembly of amphiphilic di- or tri-block polymers are quite attractive and are becoming increasingly popular.[20,21] However, the method we presented here, which uses one type of conjugated polymer and introduces functional groups through cross-linking to produce Janus-like or patchy nanoparticles, to the best of our knowledge, is new. If we compare the morphologies of the nanoparticles obtained from Cu(I) and CB6-catalyzed reactions, we can see that there are significant differences between them. Multiple patches were observed on the CPNs synthesized by the Cu(I)- catalyzed click reaction. In particular, the TEM image of **P3-CPNa** (Fig. 3) clearly shows these patches. On the other hand, CB6-containing nanoparticles have regular structures, mostly with a single patch on their surface. Moreover, the sizes of nanoparticles **P1-CPNa** and **P3-CPNa** are significantly bigger than **P1-CPNb** and **P3 CPNb**, which are in good agreement with the DLS results.

Table 2 The dynamic light scattering (DLS) measurements.

	DLS diameter (mean) (nm)	Polydispersity index
P1-CPNa	130	0.17
P2-CPNa	72	0.09
P3-CPNa	166	0.09
P1-CPNb	101	0.11
P2-CPNb	71	0.11
P3-CPNb	62	0.11

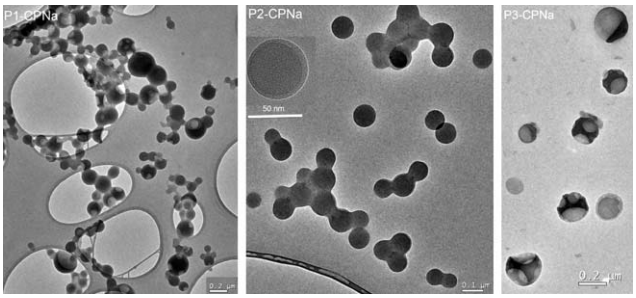

Fig. 3 TEM images of, from right to left, **P1-CPNa**, **P2-CPNa** and **P3-CPNa** synthesized by the Cu(I)-catalyzed click reaction.

In order to reveal whether the Cu(I)-catalyzed or CB6-catalyzed 1,3-dipolar cycloadditions were successful, we utilized FT-IR spectroscopy. FT-IR spectra of the nanoparticles are illustrated in Fig. 5. The samples were prepared by concentrating the nanoparticle solution and then dropping them onto a clean silicon substrate. After drying the substrate, the IR spectra were recorded. In the IR spectra, one of the characteristic peaks is the azide peak at 2090 cm^{-1}. Its intensity should decrease upon formation of the triazole ring. In all the reactions, a significant decrease in the triazole peak intensity was observed indicating that the click reactions were successful.

CB6 not only acted as a catalyst to perform the copper-free click reaction but also took part in the formation of the rotaxanes. Rotaxane formation was confirmed by FT-IR spectroscopy. Since copper was not used as a catalyst and the reaction was carried out at room temperature, a decrease in the intensity of the azide bond stretching in the FT-IR spectrum must be due to the formation of the triazole ring catalyzed by CB6. As shown in Fig. 1b, in order to explain the mechanism of the CB6-catalyzed click reaction, the triazole ring forms inside the cavity of CB6 and remains bound to CB6 due to ion–dipole interactions between the ammonium ions and the carbonyl oxygens of CB6. Moreover, in the FT-IR spectra of **P1-CPNb**, **P2-CPNb** and **P3-CPNb** (Fig. 5d, e and f), the carbonyl stretching band can be seen around 1730 cm^{-1} due to CB6. These results clearly confirm that CB6 catalyzes the 1,3-dipolar cycloaddition to form the triazole and remains in the nanoparticles as part of the rotaxanated structure.

In order to further investigate whether the 1,3-dipolar cycloaddition took place, nanoparticles were prepared in D_2O and ^{1}H-NMR spectra were recorded; however, in the ^{1}H-NMR spectra only some peaks, due to the aliphatic side chain protons, were seen. The aromatic backbone protons were not detected because the mobility of the backbone is restricted upon folding into the nanoparticle formation. However, in the case of the

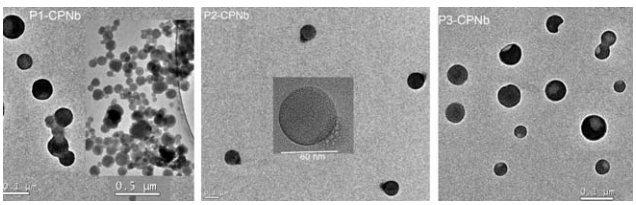

Fig. 4 TEM images of, from right to left, **P1-CPNb**, **P2-CPNb** and **P3 CPNb** synthesized by the CB6-catalyzed click reaction.

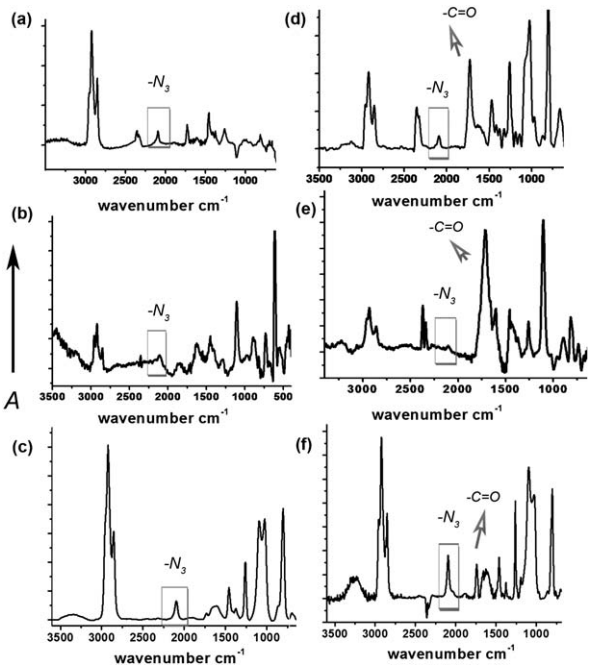

Fig. 5 The FT-IR spectra of **P1-CPNa** (a), **P2-CPNa** (b), **P3-CPNa** (c) and the CB6-catalyzed nanoparticles, **P1-CPNb** (d), **P2-CPNb** (e) and **P3-CPNb** (f).

nanoparticles synthesized by a CB6-catalyzed reaction, peaks due to the CB6 protons have been observed.

It was demonstrated that these cross-linked nanoparticles are stable by removing the solvent using a freeze-dryer and re-dispersing them in water. Optical and imaging data confirm that the re-dispersed particles preserve their shape and size.

Experimental

General

All reagents were purchased from Sigma–Aldrich Chemical Co. and were used as received. Cucurbit[6]uril and *N*,*N*′-di-prop-2-ynyl-propane-1,3-diamine hydrochloride were synthesized according to the literature procedure.[16c] Morphological characterization was done by scanning electron microscopy (SEM, Quanta 200 FEG SEM) and transmission electron microscopy (TEM, FEI Tecnai G2 F30). The sizes of the nanoparticles were measured by dynamic light scattering (DLS, Zetasizer Nano-ZS). Measurements were carried out at 633 nm and the laser, as a light source, was used at room temperature. The time-dependent autocorrelation function of the scattered light intensity was measured at an angle of 90°. The average particle diameters were calculated by the Marquardt method. The 21 DLS measurements were usually repeated at least three times and the average values were reported. For the optical characterization, a UV–vis spectrophotometer (Cary UV–Vis) and a fluorescence spectrophotometer (Cary Eclipse Fluorescent spectrophotometer) equipped with a xenon-lamp as the excitation source were used. For the structural characterization, nuclear magnetic resonance (NMR, Bruker Avance III 400 MHz spectrometer) and FT-IR (Bruker TENSOR 27) were performed. Each sample was dropped onto the silicon wafer. The data were recorded at 25 ± 1 °C, in the spectral range of 4000–400 cm^{-1}, by accumulating 256 scans with a resolution of 4 cm^{-1}. To investigate the structural changes during nanoparticle formation, nanoparticle dispersions were concentrated to increase the number of particles per unit area and a film was made by drop-casting onto the silicon substrate and then the IR spectra were recorded. To prepare the nanoparticles, Milli-Q water (18.2 MΩ) was used and, after preparation of the nanoparticles, the dispersion was dialyzed with a regenerated cellulose tubular membrane (Cellu·Sep T3, MWCO: 12 000–14 000, dry cylinder diameter: 21.0 mm, flat width: 33 nm, length: 30 m, vol cm^{-1}: 3.47 ml). The molecular weights of the polymers were determined using gel permeation chromatography (GPC, Agilent 1200), with THF as the eluent and polystyrene as a standard.

Synthesis of poly[(9,9-dihexylfluorene)-*co*-(2,5-(3-bromoethylthiophene) (P-P2)

2,5-Dibromo-3-(2-bromoethyl)thiophene **M2** (500 mg, 1.43 mmol), the boronic ester of fluorene **M3** (720 mg, 1.43 mmol) and K_2CO_3 (1.88 g) were dried under vacuum for 30 min before the addition of degassed toluene (10 ml), water (10 ml) and THF (10 ml). The mixture was stirred under argon for 10 min and then $Pd(Ph_3)_4$ (17 mg, 0.0143 mmol) was added. After heating the resulting mixture at 80 °C for 3 h, TBAB (46 mg) was added. The reaction mixture was left to complete the reaction for a further 48 h at 80 °C under argon. For the work-up, the contents of the flask was poured into a large amount of cold methanol and the precipitate was collected by suction. The solid residue was washed with water to remove K_2CO_3 and the remaining water soluble residues were dissolved in a minimum amount of THF and precipitated into cold methanol. The solid precipitates were collected and dried under vacuum for 6 h to afford a yellow powder (715 mg, 59%). **^{1}H NMR** (400 MHz, $CDCl_3$, δ): 7.83–7.49 (m, 6H), 7.02 (s, 1H), 3.63 (t, 2H), 3.22 (t, 2H), 2.06 (t, 4H), 1.28 (m, 8H), 1.12 (m, 8H), 0.79 (t, 6H). Gel permeation chromatography (**GPC**): $M_n = 0.25 \times 10^4$ g mol^{-1}, $M_w = 3.8 \times 10^3$ g mol_{-1} (polystyrene was used as a standard).

Synthesis of poly[(9,9-dihexylfluorene)-*co*-(2,5-(3-azidoethylthiophene)] (P2)

To a solution of **P-P2** (300 mg, 0.56 mmol) in DMF (10 ml) NaN_3 (56 mg, 0.862 mmol) was added, and the mixture was stirred overnight at 90 °C. After the solvent was removed under vacuum, the residue was dissolved in THF (10 ml) and the solution was precipitated into cold water (150 ml). The precipitates were collected under suction and dried under vacuum to yield a yellow powder (260 mg, 87%). **^{1}H NMR** (400 MHz, $CDCl_3$, δ): 7.60–7.34 (m, 6H), 7.00 (s, 1H), 3.59 (t, 2H), 2.94 (t, 2H), 2.07 (t, 4H), 1.27 (m, 8H), 1.12 (m, 8H), 0.80 (t, 6H). **GPC**: $M_n = 0.28 \times 10^4$ g mol^{-1}, $M_w = 3.9 \times 10^3$ g mol^{-1} (polystyrene was used as a standard).

Synthesis of poly[9,9-bis(3-bromopropyl)fluorene)-*co*-alt-(benzothiadiazole)] (P-P3)

2,1,3-Benzothiadiazole-4,7-bis(boronic acid pinocol ester) (411 mg, 1.06 mmol), 2,7-dibromo-9,9-bis(3-bromo-propyl)-9*H*-fluorene (566 mg, 1.06 mmol) and K_2CO_3 (1.47 g, 10.6 mmol) were

dried under vacuum for about 30 min. Then, degassed solvents, THF (10 ml), water (10 ml) and toluene (10 ml) were added into the mixture under argon gas. Then, the catalyst, tetrakis(triphenylphosphine)palladium [$Pd(PPh_3)_4$] was added quickly. After 3 h stirring of the mixture under argon at 80–90 °C, the phase transfer catalyst, tetra-*n*-butylammonium bromide (TBAB) was added. The stirring was continued for another 48 h at 80–90 °C to complete the polymerization reaction. For the work up, the mixture was evaporated under vacuum to obtain a solid residue, which was suspended in water; the water insoluble particles were collected by suction and dissolved in THF (15 ml) and the solution was precipitated into cold methanol (200 ml). The precipitates were collected by suction and dried under vacuum for 6 h (547 mg, 56%).

Synthesis of poly[9,9-bis(3-azidopropyl)fluorene)-*co*-(benzothiadiazole)] (P3)

Poly[9,9-bis(3-bromopropyl)fluorene)-*co*-alt-(benzothiadiazole)] (100 mg, 0.185 mmol) and NaN_3 (26 mg, 0.400 mmol) were dissolved in DMF (6 ml) and the mixture was refluxed for 24 h. After the reaction was over, the mixture was precipitated into cold methanol (100 ml). The precipitates were collected by suction and dried under vacuum (80 mg, 80%). **^{1}H NMR** (400 MHz, $CDCl_3$, δ) 7.99 (m, 8H, Ar-H), 3.26 (q, 4H, CH_2N_3), 2.41 (q, 4H, CH_2), 1.25 (m, 4H, CH_2), 0.81 (m, 6H, CH_3). **GPC**: $M_n = 4.5 \times 10^3$ g mol^{-1}, $M_w = 1.1 \times 10^4$ g mol^{-1} (polystyrene was used as a standard).

Preparation of the nanoparticles

In a typical nanoparticle synthesis using Cu(I) as the catalyst (for P1-CPNa, P2-CPNa and P3-CPNa). The polymer (6.68×10^{-3} mmol) was dissolved in THF (10 mL) and the solution was filtered through a 0.45 μm syringe filter. *N*,*N*′-di-prop-2-ynyl-propane-1,3-diamine hydrochloride (1.34×10^{-3} mmol) was dissolved in water (500 ml) and, subsequently, $CuSO_4$ (0.26×10^{-3} mmol) and ascorbic acid (0.26×10^{-3} mmol) were added to this solution. The filtered polymer solution in THF was injected rapidly into the above solution under vigorous stirring. The resulting mixture was stirred with sonication for another 1 h at room temperature and then the dispersion was left overnight at room temperature. THF was removed under reduced pressure. Some sample was reserved for the DLS analysis and the remaining solution was further concentrated to a total volume of 100 ml and was dialyzed using a 14 kDa MWCO regenerated cellulose membrane for 24 h to remove the catalyst and any unreacted species.

In a typical nanoparticle synthesis using CB6 as the catalyst (for P1-CPNb, P2-CPNb and P3-CPNb). The polymer (6.68×10^{-3} mmol) was dissolved in THF (10 ml) and the solution was filtered through a 0.45 μm Teflon syringe filter. *N*,*N*′-di-prop-2-ynyl-propane-1,3-diamine hydrochloride (1.34×10^{-3} mmol) was dissolved in water (5 ml) and CB6 (2.67×10^{-3} mmol) was added. The mixture was stirred for 30 min to obtain a clear solution and filtered through a 0.45 μm syringe filter; its volume was made up to 500 ml by adding deionized water. The filtered polymer solution in THF was injected rapidly into the above solution under vigorous stirring. The resulting mixture was stirred with sonication for another 1 h at room temperature and, then, the dispersion was left overnight at room temperature. THF was removed under reduced pressure. Some sample was reserved for the DLS analysis and the remaining solution was further concentrated to a total volume of 100 ml and was dialyzed using a 14 kDa MWCO regenerated cellulose membrane for 24 h to remove the excess CB6 and any unreacted species.

Conclusions

In conclusion, we reported a novel and facile synthetic method for the preparation of cross-linked, conjugated polymer nanoparticles possessing useful functionalities, such as triazole and amine groups. These nanoparticles can be utilized in biological studies, such as cell imaging and the attachment of biomolecules or drugs. Incorporation of the hydrophilic functional groups to the hydrophobic conjugated polymers resulted in a distinct phase separation producing Janus-like or patchy particles. CB6 not only acted as a catalyst to perform the copper-free click reaction but also took part in the formation of rotaxane-containing nanoparticles. The rotaxane formation was confirmed by FT-IR spectroscopy.

Currently, we are working to explore the applications of these intriguing nanoparticles in cell imaging and theranostic nanomedicine.

Acknowledgements

Support by TUBITAK 110T219 is gratefully acknowledged.

Notes and references

1 (*a*) D. Tuncel and H. V. Demir, *Nanoscale*, 2010, **2**, 484; (*b*) K. Landfester, *Angew. Chem., Int. Ed.*, 2009, **48**, 4488; (*c*) J. Pecher and S. Mecking, *Chem. Rev.*, 2010, **110**, 6260.
2 (*a*) C. Wu, C. Szymanski and J. McNeill, *Langmuir*, 2006, **22**, 2956; (*b*) C. Wu, C. Szymanski, Z. Cain and J. McNeill, *J. Am. Chem. Soc.*, 2007, **129**, 12904; (*c*) C. Wu, B. Bull, C. Szymanski, K. Christensen and J. McNeill, *ACS Nano*, 2008, **2**, 2415; (*d*) J. Yu, C. Wu, S. Sahu, L. Fernando, C. Szymanski and J. McNeill, *J. Am. Chem. Soc.*, 2009, **131**, 18410; (*e*) I. O. Ozel, T. Ozel, H. V. Demir and D. Tuncel, *Opt. Express*, 2010, **18**, 670–684; (*f*) I. O. Huyal, T. Ozel, D. Tuncel and H. V. Demir, *Opt. Express*, 2008, **16**, 13391–13397.
3 T. L. Andrew and T. M. Swager, *Macromolecules*, 2011, **44**, 2276.
4 M. C. Baier, J. Huber and S. Mecking, *J. Am. Chem. Soc.*, 2009, **131**, 14267.
5 C. Wu, B. Bull, K. Christensen and J. McNeill, *Angew. Chem., Int. Ed.*, 2009, **48**, 2741.
6 (*a*) J. H. Moon, W. McDaniel, P. MacLean and L. E. Hancock, *Angew. Chem., Int. Ed.*, 2007, **46**, 8223; (*b*) J. H. Moon, P. MacLean, W. McDaniel and L. F. Hancock, *Chem. Commun.*, 2007, 4910.
7 (*a*) P. Howes, R. Thorogate, M. Green, S. Jickells and B. Daniel, *Chem. Commun.*, 2009, 2490; (*b*) P. Howes, M. Green, A. Bowers, D. Parker, G. Varma, M. Kallumadil, M. Hughes, A. Warley, A. Brain and R. Botnar, *J. Am. Chem. Soc.*, 2010, **132**, 9833; (*c*) Z. Hashim, P. Howes and M. Green, *J. Mater. Chem.*, 2011, **21**, 1797.
8 C. Wu, Y. Jin, T. Schneider, D. R. Burnham, P. B. Smith and D. T. Chiu, *Angew. Chem., Int. Ed.*, 2010, **49**, 9436.
9 C. Wu, T. Schneider, M. Zeigler, J. Yu, P. G. Schiro, D. R. Burnham, J. D. McNeill and D. T. Chiu, *J. Am. Chem. Soc.*, 2010, **132**, 15410.
10 F. Ye, C. Wu, Y. Jin, Y.-H. Chan, X. Zhang and D. T. Chiu, *J. Am. Chem. Soc.*, 2011, **133**, 8146.
11 J. Pecher, J. Huber, M. Winterhalder, A. Zumbusch and S. Mecking, *Biomacromolecules*, 2010, **11**, 2776.

12 P. K. Kandel, L. P. Fernando, P. C. Ackroyd and K. A. Christensen, *Nanoscale*, 2011, **3**, 1037.
13 J. Xie, S. Lee and X. Chen, *Adv. Drug Delivery Rev.*, 2010, **62**, 1064.
14 E.-J. Park, T. Erdem, V. Ibrahimova, S. Nizamoglu, H. V. Demir and D. Tuncel, *ACS Nano*, 2011, **5**, 2483.
15 (*a*) K. Kim, N. Selvapalam, Y. H. Ko, K. M. Park and D. Kim, *Chem. Soc. Rev.*, 2007, **36**, 267; (*b*) L. Isaacs, *Chem. Commun.*, 2009, 619.
16 (*a*) D. Tuncel, H. B. Tiftik and B. Salih, *J. Mater. Chem.*, 2006, **16**, 3291; (*b*) D. Tuncel, O. Ozsar, H. B. Tiftik and B. Salih, *Chem. Commun.*, 2007, 1369; (*c*) D. Tuncel and M. Katterle, *Chem.–Eur. J.*, 2008, **14**, 4110; (*d*) G. Celtek, M. Artar, O. A. Scherman and D. Tuncel, *Chem.–Eur. J.*, 2009, **15**, 10360; (*e*) D. Tuncel, M. Artar and S. B. Hanay, *J. Polym. Sci., Part A: Polym. Chem.*, 2010, **48**, 4894; (*f*) D. Tuncel, O. Unal and M. Artar, *Isr. J. Chem.*, 2011, **51**, 525.
17 (*a*) I. O. Huyal, U. Koldemir, T. Ozel, H. V. Demir and D. Tuncel, *J. Mater. Chem.*, 2008, **18**, 3568; (*b*) I. O. Huyal, T. Ozel, U. Koldemir, S. Nizamoglu, D. Tuncel and H. V. Demir, *Opt. Express*, 2008, **16**, 1115.
18 (*a*) P. Taranekar, Q. Qiao, H. Jiang, I. Ghiviriga, K. S. Schanze and J. R. Reynolds, *J. Am. Chem. Soc.*, 2007, **129**, 8958; (*b*) J. Choi, C. R. Ruiz and E. E. Nesterov, *Macromolecules*, 2010, **43**, 1964; (*c*) J. Finden, T. K. Kunz, N. R. Branda and M. O. Wolf, *Adv. Mater.*, 2008, **20**, 1998.
19 A. Walther and A. H. E. Müller, *Soft Matter*, 2008, **4**, 663.
20 Y. Huang, J. Wang, J. Zhou, L. Xu, Z. Li, Y. Zhang, J. Wang, Y. Song and L. Jiang, *Macromolecules*, 2011, **44**, 2404.
21 T. Higuchi, A. Tajima, K. Motoyoshi, H. Yabu and M. Shimomura, *Angew. Chem., Int. Ed.*, 2008, **47**, 8044.

